



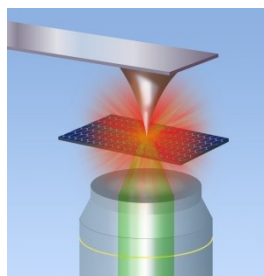
Nanoscale optical spectroscopy: an emerging tool for the characterization of graphene and related 2-D materials

Andrew J. Pollard,^{1*} Naresh Kumar,¹ Alasdair Rae,¹ Sandro Mignuzzi,¹ Weitao Su,^{2,3} Debdulal Roy^{1*}

¹National Physical Laboratory, Hampton Road, Teddington, Middlesex, TW11 0LW, UK ²Institute of Material Physics, Hangzhou Dianzi University, 310018, Hangzhou, China ³Ningbo Institute of Materials Technology & Engineering, Chinese Academy of Sciences, 315201, Ningbo, China.

Received Date: 04-July-2014

ABSTRACT



Graphene and related two-dimensional (2-D) materials have opened up new frontiers in materials science that can potentially lead to more efficient and cost-effective devices for a range of applications. In this article we provide a comprehensive description of real surfaces of 2-D materials, namely graphene and transition metal dichalcogenides, along with key spectroscopic techniques used for structural and chemical characterisation of these materials and review the recent progress and future possibilities for the use of nanoscale spectroscopy tools in investigating these 'all-surface' materials to characterize disorder, contamination, edge-effects and electronic properties.

Keywords: Raman spectroscopy, tip-enhanced Raman spectroscopy (TERS), photoluminescence, defects, contamination, 2-D materials

INTRODUCTION

The unique characteristic of all types of 2-D materials is the accessibility of the whole of the surface, as they are atomically thick. This allows the tailoring of electronic properties for advanced applications through suitable engineering processes, but also limits realistic commercialisation prospects since undesired environmental factors, such as surface contamination, can be

problematic. Optical spectroscopy tools, including Raman and infra-red spectroscopy, have played a key role in understanding chemical compositions and structures even though these readily available commercial techniques have only diffraction-limited spatial resolutions¹⁻³ and both electron microscopy and scanning probe microscopy techniques have been the main tool to conduct nanoscale investigations.^{4,5} In this regard, near-field microscopes are still not wide-spread enough, even though scanning near-field optical microscopy (SNOM) has been reported since the 1980s by Betzig *et al.*⁶ and Zenhausern *et al.*,⁷ and various groups have championed this and related techniques to extract nanoscale optical contrast and dielectric properties.^{8,9} The research activities in near-field spectroscopy have since expanded into new techniques following this research, first using probes with an aperture and then apertureless scattering-type probes. This led to detailed nanoscale chemical information being obtained, through tip-enhanced Raman spectroscopy (TERS), first reported by

Corresponding Author: Dr. Andrew J. Pollard and Dr. Debdulal Roy
Tel:
Email: andrew.pollard@npl.co.uk, debdulal.roy@npl.co.uk

Cite as: *J. Mat. NanoSci.*, 2014, 1(1), 39-49.

©IS Publications

Zenobi¹⁰ and Kawata,¹¹ Pettinger¹² and Anderson¹³ in 2000. TERS offered two major advantages over SNOM - (a) it provides full spectroscopic information facilitating chemical analysis, and (b) the artefacts arising due to cross-talk with the topography were reduced since inelastically scattered photons were detected at a different wavelength from the excitation beam.^{14,15} Tip-enhanced Raman spectroscopy has been applied on a range of materials including single molecules,¹⁶ 1-D nanostructures such as carbon nanotubes and nanowires,¹⁵ polymer thin films¹⁷ and 2-D materials such as graphene.^{18,19} Amongst these, 2-D materials, which include graphene and graphene-like materials such as transition metal dichalcogenides (TMDs), have drawn significant attention because of their technological potential to be used in nanoelectronics, and both nano-optical and nanomechanical devices. TERS is a powerful nanoscale technique for characterization of these ‘all-surface’ materials with spatial resolution of a few tens of nanometres or less. In this article, we describe the issues of disorder and contamination in real-world 2-D materials before focussing on the spectroscopic imaging capabilities for characterising 2-D materials. The challenges facing tip-enhancing techniques are also outlined, as is a guideline to the standards and reference samples required to advance these nanoscale techniques. Recent scientific reports on the mapping of graphene and MoS₂ are outlined, and finally the potential use of advanced non-linear optical techniques with nanoscale resolution is discussed.

2. DEFECTS AND CONTAMINATION CHALLENGES FOR 2-D MATERIALS

For graphene and other graphene-like 2-D materials, both the level of disorder and the surface contamination present are key considerations in advancing these materials from research environments to real-world applications.

Over the last decade of investigation into 2-D materials, techniques such as transmission electron microscopy (TEM), scanning tunnelling microscopy (STM) and Raman spectroscopy have been extensively used to visualise and probe the disorder present in graphene,²⁰⁻²⁴ and reveal the different types of lattice defects. These include vacancy defects,^{22,24,25} dislocation defects,^{20,26} line defects or grain boundaries,^{27,28} edge defects,^{19,29} charge defects,³⁰ corrugation,^{28,31,32} atomic substitution^{33,34} and *sp*³-bonding defects.^{35,36} Terminology is particularly important, as ‘defect’ in the classical sense may refer to a large-scale non-uniformity or breakage and this term may broadly be used for the same type of features in graphene-based products. However, this classical terminology is not considered the same as the previously listed types of ‘graphene defects’ which are typically on the nanoscale. Figure-1 shows TEM and STM images of examples of dislocation and vacancy defects, revealing the capability of these characterisation techniques to resolve the nanoscale changes in the graphene lattice due to the deformation of up to four carbon rings or removal of one carbon atom. It should be noted that graphene defects are not necessarily undesired, as the term ‘defect’ is typically seen as negative, and may in fact be key to enabling applications. Examples of such applications are vacancy defects introduced into graphene to enable liquid filtration and desalination,^{21,37} the introduction of

non-carbon elemental or molecular species through doping for electronic applications³³ and graphene functionalisation for polymer-composites.³⁸ Contrastingly, the supreme conductivity of graphene is a desired property for many electronic applications, and this conductivity is reduced by the introduction of disorder due to scattering processes.^{32,39}

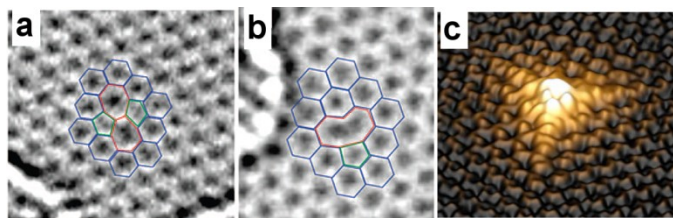


Figure 1. Visualising dislocation and vacancy defects in graphene. (a) ATEM image of a Stone-Wales dislocation defect with an overlay of the atomic structure as a guide to the pentagon and heptagon carbon rings and (b) TEM image of a single vacancy defect with a corresponding overlay, both from Ref 20, Copyright 2008 American Chemical Society. (c) A 3-DSTM topography image of a single vacancy defect, measured at 6K, tunnelling current 0.5 nA with sample bias of +150 mV, from Ref 22, Copyright 2010 American Physical Society.

Contamination is a critical problem in the commercialisation of 2-D materials, in the form of adventitious contamination from ambient conditions or as a result of processing of these materials and subsequent devices. Due to the essentially all-surface nature of these 2-D materials, surface contamination can drastically reduce the supreme properties that these exciting materials possess. This is a challenge commonly encountered within the academic community, but under-investigated due to both the difficulty in reliably characterization or removing the undesired chemical species and the reduced requirement of reproducibility in a blue-sky research environment as compared to the needs of industrial production. The nanoscale visualisation of organic molecules purposefully introduced on graphene single-layers (ILGs) has previously been achieved,^{40,41} however it is by far more challenging to truly define the exact chemical species present on the surface of 2-D materials due to exposure to ambient conditions or material processing.

Chemical vapour deposition (CVD) is recognised as the most likely fabrication method for producing large-area single-layer graphene⁴²⁻⁴⁴ that will both be suitable for electronic applications and industrial mass-production. This production process has also been used to produce other 2-D materials, such as hexagonal boron-nitride single-layers.^{45,46} However, CVD graphene must be transferred from the metal substrate used for growth, onto an application-specific substrate typically using a sacrificial polymer layer. Although this polymer is then etched away using chemical methods, as shown in Figure 2a, the polymer is not entirely removed; instead an inhomogeneous nanoscale-thick layer is left on the sample. The subsequent inhomogeneity of adsorbed species on the surface of a 2-D material is particularly disruptive for electronic applications due to scattering processes³⁹ and can substantially affect the conductivity and doping of the 2-D material.^{47,48}

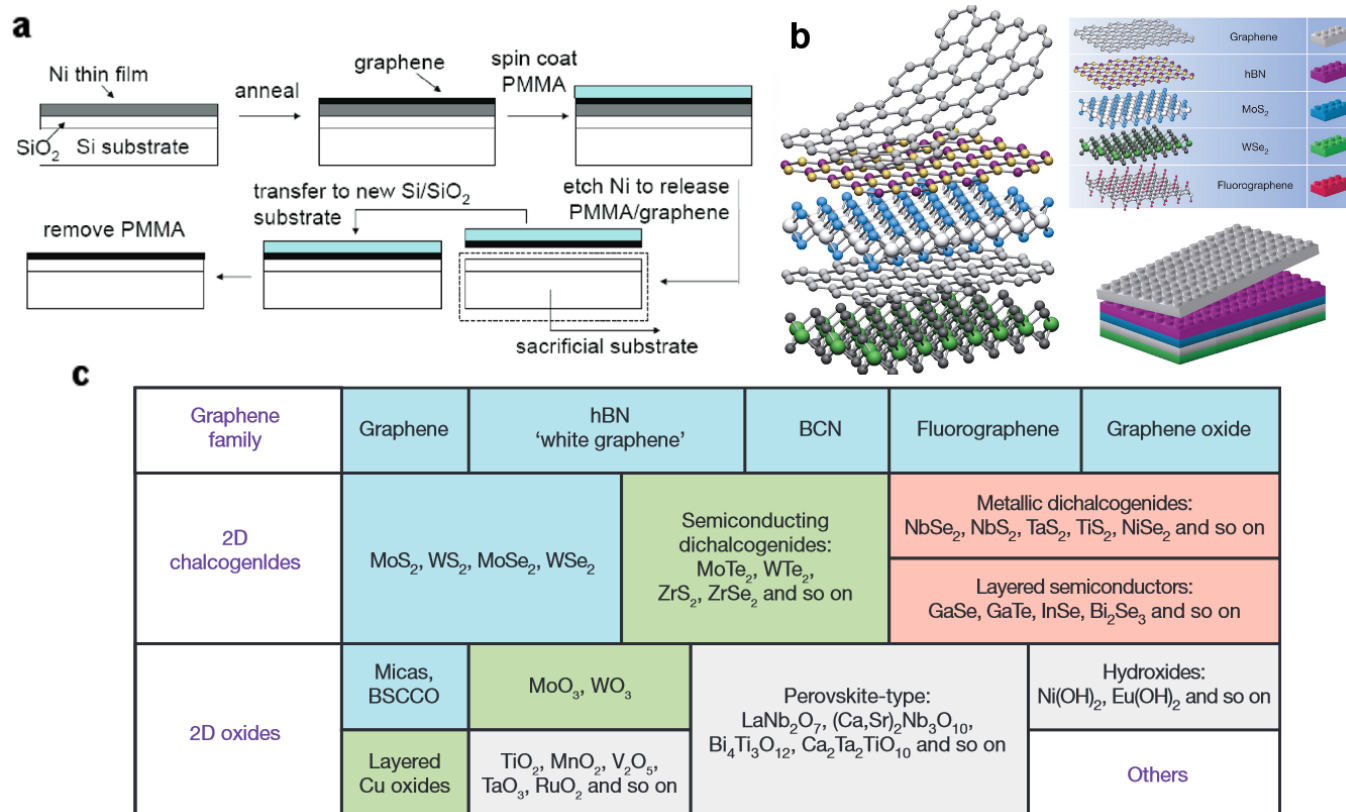


Figure 2. 2-D materials, heterostructures and CVD-transfer. (a) CVD growth and subsequent transfer of single-layer graphene from Ni thin film, via a sacrificial polymer film, from Ref 43, Copyright 2009 American Chemical Society. (b) Illustration of a 2-D material heterostructure formed from layers of different 2-D materials, (c) Table of 2-D layered material families. Both (b) and (c) were reproduced from Ref. 52, Copyright 2013 Nature Publishing Group.

The fabrication of electronic devices consisting of 2-D materials also leads to challenges in surface contamination in itself, as typical methods for creating contacts with optical lithography or electron-beam lithography requires a surface to first be covered in typically a polymer resist. This process results in creating an inhomogeneous layer of polymer residue on the surface of the 2-D material,⁴⁸ similar in scope to the residue problems caused by the transfer of CVD-grown 2-D materials.

Although 2-D materials other than graphene are now an exciting area of research, these newer materials are still very immature, even when compared to graphene itself. This is why work performed on materials such as MoS₂, WS₂, MoSe₂, WSe₂ and others shown in Figure 2c, typically involves mechanical or liquid-phase exfoliation of the bulk counterpart and therefore has associated challenges with adventitious chemical species present on the surfaces.^{49,50} This problem is exacerbated for research into the properties of heterostructures made from several different 2-D materials,^{51,52} as shown in Figure 2b, where different layers are mechanically exfoliated on top of one another in separate exfoliation processes.

To counter this contamination problem, cleaning procedures for 2-D materials have been developed, primarily by heating the samples in inert atmospheres.^{50,51,53,54} Reports vary on the success of the removal of polymer residues using these different

techniques and typically the resulting electronic properties of devices are used as the measurand, showing some improvement. However, these cleaning methods are generally accepted to make the surface 'cleaner' rather than completely clean. Only when both superior performance and the reproducible production of graphene materials and devices are reached, the commercialisation of graphene will be truly achievable in many technology areas.

Therefore, the nanoscale mapping and understanding of both defects and contaminants is required for these atomically-thin materials, with nanoscale spectroscopy an emerging tool that can enable fast, non-destructive, and reliable measurements, or in some cases a more comprehensive understanding of their non-nanoscale counterparts.

3. RAMAN CHARACTERISATION OF GRAPHENE AT THE NANOSCALE

The ever-expanding research into the inclusion of 2-D materials, such as graphene and MoS₂, in nanoscale electronic devices calls for a non-destructive measurement techniques that can characterise these materials with nanoscale resolution.⁹ However, conventional optical techniques cannot be utilised for this high resolution characterisation because of the associated diffraction-limited spatial resolution and the size constraints of these devices. The maximum spatial resolution that an optical technique such as confocal Raman spectroscopy can achieve with

an excitation laser of wavelength λ and an objective lens with numerical aperture (NA) is $(0.61\lambda)/NA$, which is not high enough to resolve features in nanoscale electronic devices. Furthermore, even though scanning probe microscopy (SPM) techniques can provide topographic mapping with an atomic resolution, these techniques cannot determine the chemical composition of the surface. Hence, development of novel optical techniques is essential to optimise the functionality and performance of nanoscale electronic devices based on graphene and 2-D materials.

In the last decade, tip-enhanced Raman spectroscopy (TERS) has been established as a powerful technique to provide simultaneous topographic and chemical information from a surface at the nanoscale, thus overcoming the limitations of both SPM and optical techniques.⁵⁵ TERS requires a metal or metal-coated SPM tip apex at the centre of a laser focus, providing an enhancement of the electric field at the tip-apex due to a combination of localised surface plasmon (LSP) resonance and the lightning rod effect.⁵⁶ A schematic of a bottom illumination AFM-TERS set-up is presented in Figure 3. The enhancement and confinement of the electric field to a region equal to the radius of the tip-apex enhances the Raman scattering signal from this nanoscale area. Once the TERS tip and laser focus are aligned, the sample can be raster-scanned and simultaneous topographic and Raman spectroscopy images produced with a resolution that is now limited by the size of the tip-apex rather than the laser wavelength. TERS has already been demonstrated in diverse areas of research ranging from organic electronics⁵⁷, material science⁵⁸ and biology,⁵⁹ and offers great potential for nanoscale characterisation of graphene and 2-D materials.

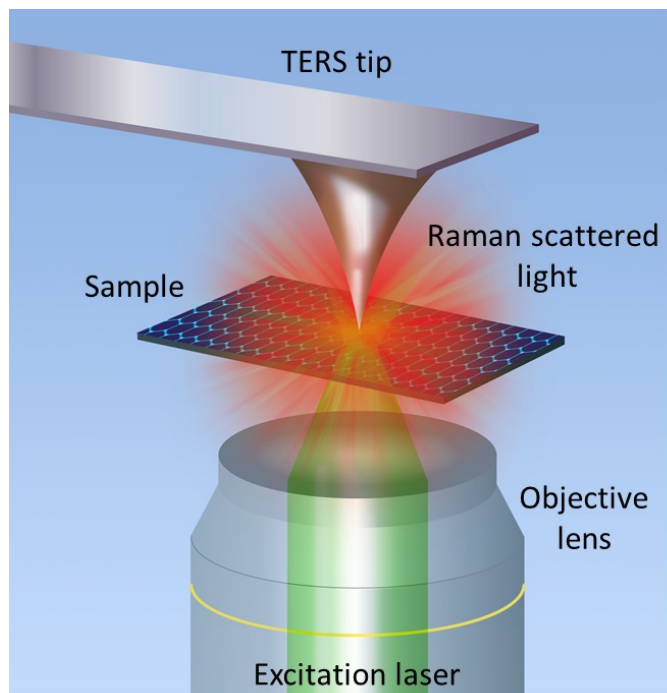


Figure 3. Schematic diagram of a bottom illumination AFM-TERS set-up. In this geometry Raman scattered photons are collected by the same objective lens that is used to excite the sample.

Stadler *et al.* have performed high resolution STM-TERS imaging of CVD-grown single-layer graphene on a Cu substrate as well as mechanically exfoliated graphene on a template-stripped Au substrate.¹⁸ A huge signal contrast of up to 80 was achieved between the near-field and far-field Raman signals and nanoscale adsorbates and defects were localised on the graphene surface with a spatial resolution <12 nm. In this study large contrasts in the maps with D-peak and the 2D-peak intensities were observed between different regions of the samples. Since the scattering from a defect takes place only from a very small area (~ 10 nm), the enhancement from the D-band originating from defects or adatoms is very high.⁶⁰ The 2-D band is also very sensitive to the local environment and contrast observed in this work is not unusual.

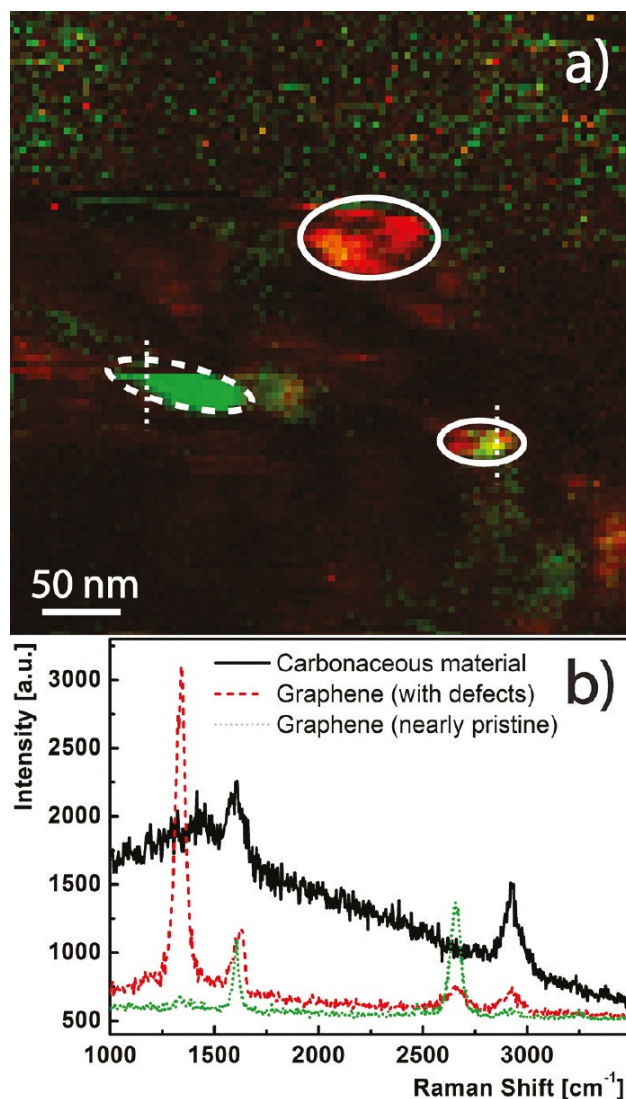


Figure 4. (a) A high resolution TERS image of graphene on a template-stripped Au substrate. Green and red colours represent the graphene 2D- and D-band intensity, respectively. Areas showing intense graphene 2D- and D-band signals are highlighted with dotted white and solid white circles, respectively. (b) TERS spectra for the graphene, defect and graphene-free regions. Both (a) and (b) were reproduced from Ref.,¹⁸ Copyright 2011 American Chemical Society.

Figure 4a shows a 100×100 pixel TERS image of a 400×400 nm² area of graphene on a template-stripped Au substrate. Green colour corresponds to the intensity of 2D-band at ~ 2670 cm⁻¹ and red colour corresponds to the intensity of D-band at ~ 1350 cm⁻¹. An area with an intense graphene signal can be seen in the image (dotted circle) surrounded by region of weaker graphene signal, which is not clearly visible due to the high contrast of the image. The full width at half-maximum (FWHM) of the intensity profile along the white dotted line marked in this area was calculated to be 10.6 nm. Two areas showing intense defect peaks can also be identified (solid white circles) with a resolution of 11.8 nm (FWHM of the dotted line on the bottom right area). Raman spectra from a graphene area, defect area and an area of carbonaceous material are shown in Figure 3b. These high resolution maps of ILG and defect areas demonstrate that TERS is an effective technique to map localised nanoscale contaminants and defects on graphene with high sensitivity, which is essential for the development of reliable electronic devices and structures based on graphene and 2-D materials.

As described in Section 2, the different classifications of graphene defects are varied. Point defects, such as single vacancies or single atomic dopants as shown in Figure 1, have a length scale of less than 1 nm. This scale is far below the spatial resolution of confocal Raman spectroscopy measurements. Although the highest resolution of TERS reported is below 1 nm,⁶¹ so far no nanoscale resolution images of point defects have been reported for graphene.

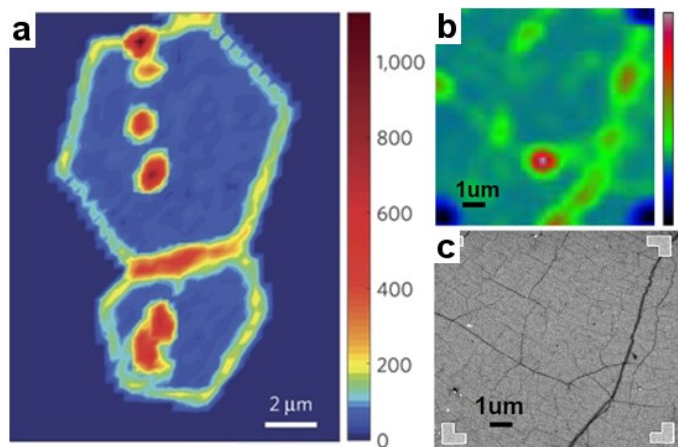


Figure 5. Confocal Raman imaging of graphene. (a) D-peak intensities around grain boundaries of CVD-grown single-layer graphene, from Ref.²⁷ Copyright 2011 Nature Publishing Group. (b) Raman D-peak intensity mapping, and (c) SEM imaging of graphene wrinkles, from Ref.⁶² Copyright 2012 American Chemical Society.

Grain boundaries act as strong carrier scattering sites, greatly decreasing the carrier mobility, and adsorbates anchored on grain boundaries may also act as *p*- or *n*-type dopants. Nanoscale measurements of these grain boundaries using high resolution TEM and conductive AFM have been previously published. However, due to the nanometre scale of grain boundaries, confocal Raman spectroscopy measurements provide images of the D-peak for these grain boundaries that are convoluted with the

probe size, as shown in Figure 5a.²⁷ This convolution effect is also seen for the Raman D-peak measured for physical wrinkles in CVD-grown graphene as shown in Figure 5b.⁶² TERS is the only potential technique that can provide nanoscale spectroscopic imaging of grain boundaries and wrinkles, though this is yet to be reported. For physical variations in the graphene lattice, the situation is more complicated as TERS systems operating in contact-AFM mode may induce physical changes in the graphene layers themselves.

Su *et al.* have reported high resolution Raman image of a graphene-edge using the D-peak intensity and calculated the electron phase-breaking length at room temperature.¹⁹ The average distance travelled by a photon excited electron-hole pair during its lifetime is defined as the phase-breaking length (L_σ).⁶³ Accurate measurement of the phase-breaking length near an edge is required to evaluate the electronic properties of graphene-edges. The D-peak originates from transverse optical (TO) phonons around the K-point in the phonon dispersion curve of graphene, and requires a defect for its activation. Probing the Raman D-peak intensity distribution across the edge of a graphene flake serves as an accessible method for determining the value of L_σ . However, because the spatial resolution of confocal Raman microscopy (>250 nm) is approximately two orders greater than the expected value of L_σ , a confocal Raman measurement will not suffice. Through TERS imaging measurements, Su *et al.* measured the minimum D-peak spatial width as 18.2 nm with nanoscale spatial resolution (16 nm),¹⁹ as shown in Figure 6. According to this result, the phase-breaking length was calculated to be ~ 4.2 nm, in good agreement with literature.^{24,25,63}

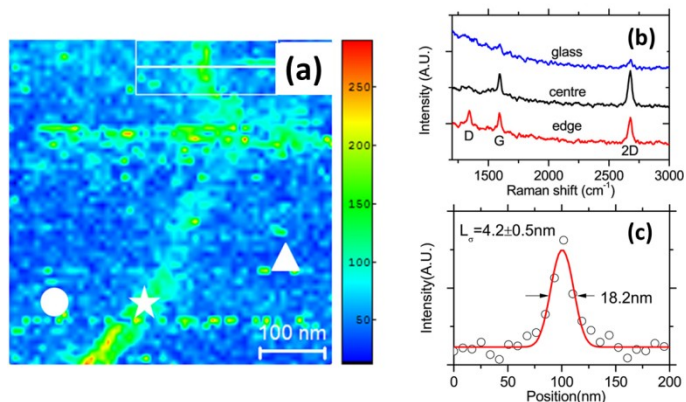


Figure 6. TERS imaging of a graphene flake. (a) TERS mapping of a graphene edge. (b) TERS spectra at three distinct positions marked in (a) as a circle (centre), star (edge) and triangle (glass). (c) (open circle) Average D-peak intensity in the rectangular marked area of (a), (solid line) calculated D-peak intensity, revealing a D-peak spatial width of ~ 18.2 nm and phase-breaking length (L_σ) ~ 4.2 nm. Adapted from Ref 19, Copyright 2013 American Vacuum Society.

Prior to this work, confocal microscopy has been used by other groups to obtain the value of L_σ .²⁹ Due to high signal-to-noise ratio in the Raman measurements, significant scattering was observed in the value of L_σ . These difficulties were partially overcome by Beams *et al.*⁶³ using defocusing methods with a

confocal microscope, combined with theoretical calculations. These measurements also determined the phase-breaking length to be ~4 nm at room temperature.

4. INSTRUMENTATION CHALLENGES OF TIP-ENHANCEMENT TECHNIQUES

For tip-enhanced nanoscale optical spectroscopy, an SPM system is coupled with a confocal microscope so that a metal or metal-coated probe can be held in close proximity to a surface¹⁵. There has been considerable improvement in automation and control of the tip-sample distance, as well as the coupling of the laser probe volume with the TERS probe. However, further developments are required in the areas of reproducibility of the TERS probes, applying a non-metallic protective layer on the probes and also reference samples for characterisation of the TERS probes themselves.

The preparation of metal or metal-coated probes is considered to be a major challenge in the implementation of tip-enhanced optical spectroscopy. The quality of the probe determines the signal enhancement that can be achieved in the near-field, which in turn determines the resolution and contrast obtainable in the tip-enhanced optical image. Hence, fabrication of highly enhancing and reproducible probes is critical for the nanoscale characterisation of graphene and 2-D materials. These metal and metal-coated probes can provide not only Raman scattering measurements, but simultaneous topography, photoluminescence and electrical information with nanoscale resolution.

Progress has been made recently in addressing the issues of tip reproducibility and yield. Yeo *et al.* obtained close to a 100% yield of Ag-coated TERS probes when they coated the AFM tip with low refractive index materials such as SiO_x and AlF₃, and achieved large contrast values of 70-80 on brilliant cresyl blue (BCB)⁶⁴. Hayazawa *et al.* have also reported a 100% yield of TERS probes with an enhancement factor >100 on single-wall carbon nanotubes (SWCNT) samples by oxidising silicon AFM tips and then coating them with Ag.⁶⁵ Decreasing the refractive index of the AFM tip prior to the metal coating improves the LSP resonance characteristics of the TERS probes, thus enhancing their overall yield and reproducibility.⁶⁴

An inert coating, such as an oxide layer, on top of the metal-coated tip would prevent degradation and contamination of the probe. Ag-coated AFM tips have been found to have superior enhancing properties, however, they soon degrade due to oxidation in ambient conditions. Moreover, the metals used for coating, such as gold and silver, are prone to wear during scanning and a coating with superior mechanical properties would reduce the mechanical damage and wear to the probe. Stable oxides such as Al₂O₃ and SiO₂ can be used as a coating material since these can be deposited as thin films of nanometre thickness. Such nonconducting oxides can also be used for measuring tip-enhanced PL imaging of 2-D materials as described in Section 4.⁶⁶

Standardised procedures and reference samples enable reproducible and accurate measurement techniques, and quantitative measurements are only possible when a measurement has a known uncertainty. Yet there are no accepted standardised procedures and reference samples to verify current nanoscale spectroscopic measurements. However, it is recognised that

standardisation in this area needs to be developed if these new techniques are to progress into industrial environments and diverse application areas. The measurement of enhancement factor (EF) is considered to be a key parameter in nanoscale spectroscopy. Bortchagovsky *et al.* have recently reported a method to remove the local variation of EF by coating TERS probes in a single-layer of chemisorbed molecules and using the near-field signal from these molecules as an internal standard.⁶⁷ This method, however, needs a plasmonic metal surface to enhance the signal from the molecule in-between the metal tip and metal surface. Roy *et al.* have reported a methodology to measure the enhancement factor of a TERS probe by imaging a SWCNT.⁶⁸ The TERS image of a SWCNT has a near-field signal overlapped on top of a far-field background that can be separated by fitting two Gaussian functions to a cross-section of the image. Hence, the true enhancement factor of the TERS tip can be calculated from the ratio of the near-field to far-field signal. Kumar *et al.* have recently reported a simpler method to estimate the enhancement factor of a TERS tip through elimination of far-field artefacts using a bilayer sample.⁶⁹ This method consists of conducting 'tip-in' and 'tip-out' measurements on a sample that consists of two thin-films with unique and distinct Raman peaks. The Raman scattering signal from the top film is plasmonically-enhanced due to the LSP resonance at the TERS probe-apex, however the signal from the bottom layer is purely due to far-field excitation, which may be increased due to the presence of the TERS probe because of scattering and multiple reflections between the tip-shaft and the sample. Thus, when the TERS probe is present, the true plasmonic-enhancement can be separated from the increase in far-field signal from the Raman scattering signals, from the top and bottom layers respectively.⁶⁹

Such reference samples are required for improving the performance of tip-enhanced optical systems, the confirmation of stability and optical alignment, and to optimise the preparation of tip-enhanced optical probes. Furthermore, they can be used to compare the contrast factor of different probes and performance of instruments through interlaboratory studies, thus enabling reproducible nanoscale spectroscopic measurements that can be applied in areas such as 2-D materials, and beyond.

5. PHOTOLUMINESCENCE AS A CHARACTERISATION TOOL FOR 2-D MATERIALS

Photoluminescence (PL) spectroscopy is progressively emerging as a tool for the characterisation of direct-gap 2-D semiconductors. This is especially true for the group 6 TMDs, i.e. MoS₂, WS₂, MoSe₂, and WSe₂, which are indirect gap semiconductors in the bulk form, but found to be direct gap semiconductors when in their single-layer form.⁷⁰⁻⁷² The shape, position and relative intensity of PL peaks are valuable quantities which can be directly correlated to the electronic and structural properties of the atomically thin TMDs.

The electronic band structure is fully captured in the PL spectrum, becoming an immediate tool to probe the number of layers.⁷⁰ Two PL peaks are usually present in few-layer samples, respectively associated to the direct (A) and to the indirect (I) exciton transitions.⁷² The strong intensity of the A peak is a direct signature of single-layer.⁷¹ Its intensity progressively decreases

upon increasing the number of layers, accompanied by a downshift of the I-peak energy.⁷⁰ In MoS₂, the strong spin-orbit band splitting (148 eV)⁷³ is also responsible for two possible direct transitions, named A and B.⁷⁰

Compared with few-layers, the reduced dielectric screening in isolated single-layers makes the Coulombic interactions stronger, giving rise to tightly bound trions.⁷⁴ As a consequence, a new PL peak is observed at the lower side of A (Figure 7), and associated to negatively charged trions A⁻ (quasiparticles composed by two electrons and one hole).⁷⁴ Its intensity is enhanced in the presence of an excess of electrons, as emerged from gate-induced doping experiments.⁷⁴ Such sensitivity permits an easy assessing of doping, which is of primary importance in 2-D materials, whose carrier concentration is strongly affected by the environment. For instance, systematic studies have been carried out on single-layer MoS₂ supported by dielectric and conducting substrates,^{75,76} in the presence of dielectric capping,⁷⁶ and suspended,⁷⁷ showing the sensitivity of PL spectroscopy in detecting different charging effects.

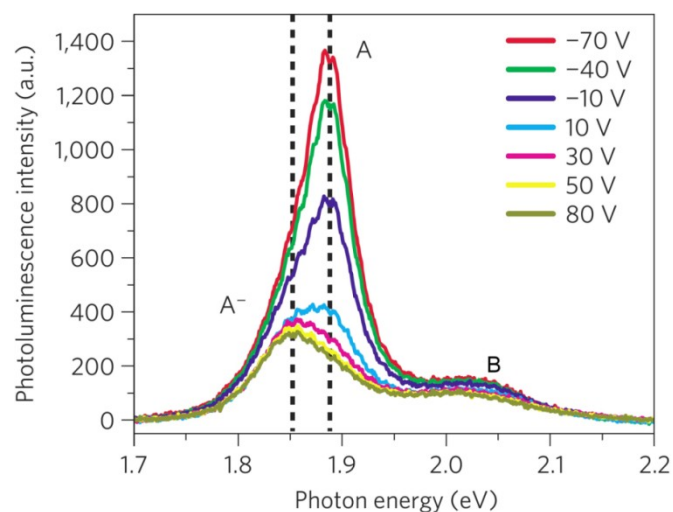


Figure 7. PL spectra of single-layer MoS₂ at different gate voltages. The energy of the neutral exciton (A) and the trion (A⁻) are indicated by dashed lines. The additional peak, usually referred to as B, is due to the direct transition involving the lower split valence band. Adapted from Ref. 74 Copyright 2013 Nature Publishing Group.

The dimensionality confinement along the out-of-plane direction make the band structure, and consequently PL, easily affected by defects.⁷⁸ This has made PL spectroscopy widely used to characterise the level of disorder and the crystallinity of CVD-grown TMDs. PL inhomogeneities have been reported in as-grown flakes both in MoS₂⁷⁹ and WS₂.^{80,81} PL intensity has indeed been reported to undergo quenching at grain boundaries of MoS₂⁷⁹ and enhancement at WS₂ edges,⁸⁰ and has been shown to depend on the growth process.⁸¹ The effect of defects has been studied for oxidised flakes of MoS₂⁸² and also α -particle irradiation of MoS₂, MoSe₂ and WS₂.⁸³ In these cases of induced disorder, an enhancement of PL has been observed^{82,83} (see Figure 8), along with PL emissions at new energies.⁸³ This variation of results arise due to a combination of different factors, such as appearance of

new discrete gap states,^{78,83} doping by adsorbates⁸⁴ and oxidation.⁸² Defects can also induce strain, which can modify the optical emission. Indeed, the band structure of atomically thin TMDs is easily modulated by uniaxial^{85,87,88} and biaxial⁸⁹ strain, permitting an easy engineering of optical and electronic properties.⁹⁰

Aperture-less near-field optical microscopy through the enhancement of LSPs may be a promising technique for characterising 2-D dichalcogenides. Although the highest spatial resolution (~ 10 nm)¹⁸ is larger than the size of most defects and adsorbates, near-field optical microscope is still potentially useful for investigating the localised electronic properties caused by defects and adsorbates; however, no tip-enhanced Raman or PL of 2-D dichalcogenides has yet been reported, possibly due to a number of challenges.

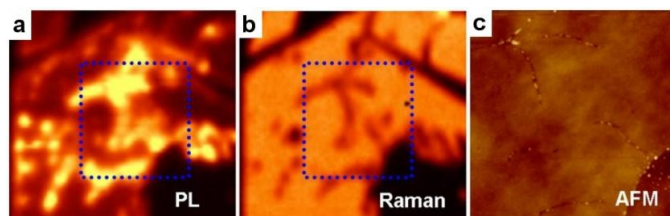


Figure 8. (a) PL, (b) Raman and (c) AFM maps of cracks in high-temperature annealed single-layer MoS₂. Bright zones in the PL map refer to the enhanced optical emission at defect sites. Adapted from Ref. 82, Copyright 2014 American Chemical Society.

It is well understood that 2-D dichalcogenides are much more susceptible to damage via laser irradiation than graphene. Thus, the confocal PL or Raman measurements for 2-D dichalcogenides are typically conducted with lower laser powers of <200 μ W or lower, depending on the objective lens used,^{71,91,92} to avoid thermal damage. The highly localised electric field under the metal or metal coated tip-apex is also many times higher than the incident electric field.^{19,69} Taking the case of an enhancement contrast of 2 as an example, for an oil immersion objective lens with NA=1.49, laser wavelength=532 nm, and a typical tip-apex radius of 25 nm, the electric field under the tip-apex is enhanced by a factor of 10 or more. In ambient conditions, such a strong electric field will oxidise the 2-D flake very quickly during any imaging process. Other options would be to either use a probe with poorer enhancement or by further decreasing the laser excitation power, however neither of these options will benefit the viability of TERS measurements since the Raman scattering signal of single-layer 2-D dichalcogenides is very weak. By pursuing a lower laser power or lesser enhancement the Raman scattering signal to noise ratio will also be decreased, which will in turn render the measurements ineffective at obtaining any electronic information. TERS mapping in an inert environment or ultrahigh vacuum^{93,94} may inhibit damage caused during imaging measurements.

Since the PL signal of 2-D dichalcogenides is always of significant intensity, tip-enhanced PL may be an applicable technique in ambient conditions. However, the key challenge may be the quenching of the PL signal at the metallised tip-apex due to

the localised energy transfer between the tip and 2-D semiconductor. Using a perfectly symmetric tip where the enhancement hotspot and PL quenching point spatially coincide at the tip-apex may in fact lead to no observable PL enhancement.⁹⁵⁻⁹⁷ One possible solution could be to coat the metallic tip with a few-nanometre thick layer of insulator, such as SiO₂ or Al₂O₃,⁹⁸ which would retain the probe enhancement but exclude the quenching effect. Therefore, tip-enhanced PL measurements with nanoscale resolution are still possible by addressing the aforementioned challenges.

6. PROBING THE PROPERTIES OF 2-D MATERIALS WITH SECOND HARMONIC GENERATION

Alongside their unusual electrical and mechanical properties, 2-D materials also exhibit unusual non-linear optical response in comparison with their bulk counterparts. As such, non-linear optical phenomenon can be an excellent probe of physical structure, band structure, number of layers, doping and electrical field effects in 2-D systems. This section briefly summarises the use of SHG as a probe of structure in 2-D materials and explores the prospects for nanoscale nonlinear measurements. Due to its centrosymmetric structure, SHG is intrinsically forbidden in free-standing graphene single-layers.⁹⁹ However, this symmetry is broken by the presence of a substrate, allowing the generation of second harmonic radiation.¹⁰⁰ It is found that SHG in graphene exhibits a dependence on both the number of layers and the azimuthal angle of rotation about the normal of the substrate.¹⁰¹ This makes SHG a powerful probe of structure in graphene films. Indeed, SHG has been used to probe structural inhomogeneities in graphene, revealing the presence of wrinkles.¹⁰²

SHG can also be a powerful probe of the extrinsic properties of few-layer graphene structures. It has been found that the presence of a DC field can enhance SHG from graphene on various substrates.⁹⁹ Due to the variation of current-induced SHG with the measurement location along the direction of current flow,⁹⁹ SHG could be a powerful probe of charge distribution in graphene devices.

It is clear that SHG can be a useful probe of both the intrinsic and extrinsic properties of graphene. However, graphene is not the only 2-D material that exhibits a useful nonlinear optical response. Unlike graphene and its bulk parent structure, single-layer and other odd layered structures of MoS₂ are non-centrosymmetric. This is reflected by a large increase in the second harmonic response for odd layered structures of the material. The orientation dependence of the SHG emission reflects the 3-fold rotational symmetry of the structure (Figure 9). This allows SHG to be used as a powerful probe of crystallographic orientation in MoS₂¹⁰³ as well as h-BN.¹⁰⁴

Although all of these measurements probe the bulk properties of graphene and other similar 2-D materials, there is great potential for nanoscale nonlinear optics. SHG beyond the diffraction limit has been demonstrated on ZnO nanowires using tip-enhanced SHG.¹⁰⁵ Using a SNOM configuration with an ultrafast Ti:sapphire regenerative amplifier, the authors demonstrated SHG mapping of a single ZnO nanowire. Sub-diffraction limited imaging of this structure revealed inhomogeneities in material properties undetectable by other

techniques. For example, the authors observed <100 nm variations in the SHG intensity which could be attributed to crystallographic domain alignment or surface contamination, as shown in Figure 10. A passivation study on the same ZnO nanowire system revealed a much reduced SHG intensity owing to the centrosymmetric nature of the passivation layer. This highlights the utility of tip-enhanced SHG in nanoscale surface-specific contamination studies.

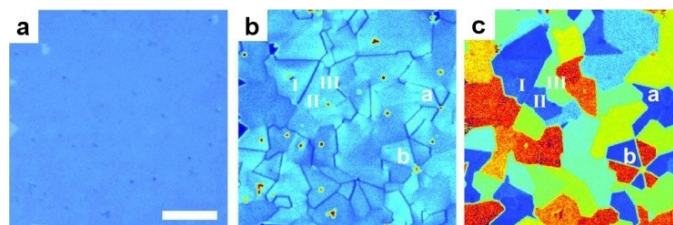


Figure 9. SHG imaging of MoS₂. (a) Optical image of single-layer CVD-grown MoS₂. (b) Second harmonic image of the same area, boundaries between grains are clearly identified by the reduced second harmonic intensity. (c) Crystallographic orientation of the single-layer MoS₂ flakes derived from SHG signal. From Ref. 103, Copyright 2014 AAAS.

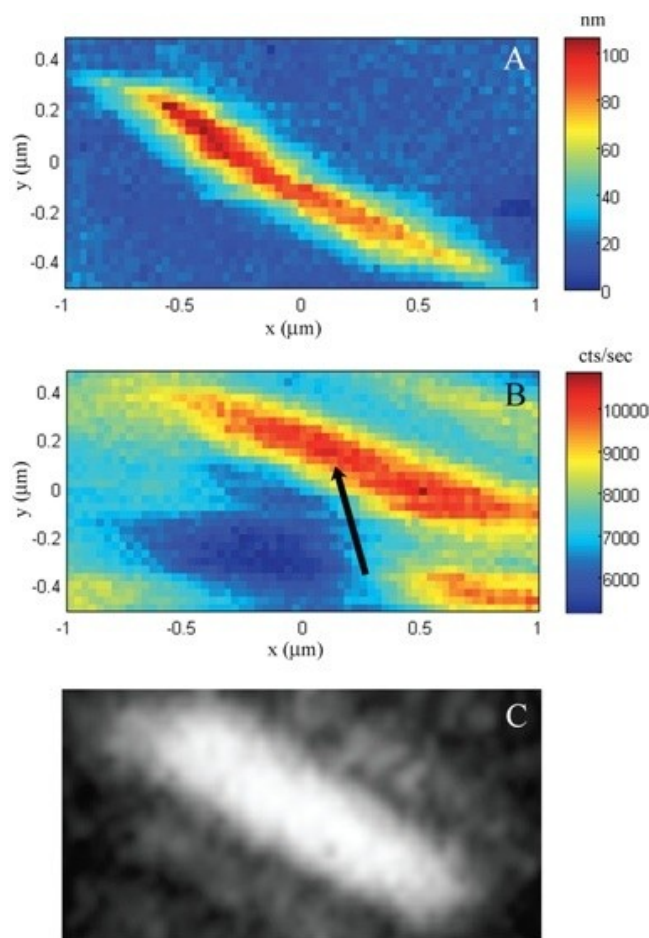


Figure 10. (A) AFM, (B) tip-enhanced SHG and (C) far field SHG images of a single ZnO nanowire on fused silica. Each image is 64x32 pixels with a 1 second integration time per pixel. From Ref 105, Copyright 2014 Society for Applied Spectroscopy.

Although tip-enhanced SHG studies are rare, there are exciting possibilities to use tip-enhanced SHG to probe the local symmetry breaking induced by defects and edge states in the new generation of 2-D material structures. With the aid of a growing knowledge in the field of tip-enhanced Raman spectroscopy, tip-enhanced SHG is a promising tool for the nanoscale study of the structural properties of 2-D materials.

CONCLUSION

We have summarised the characterisation needs to investigate contamination and defects for graphene surfaces, and the role that emerging nanoscale spectroscopic techniques based on tip-enhanced Raman spectroscopy can play in understanding these 'all surface' materials. Both surface contamination and lattice disorder alter the electronic properties of single-layer 2-D materials, which can be measured by the Raman peak positions and intensities, as well as photoluminescence arising from electronic transitions in case of semiconducting materials. TERS instruments enable to capture these signals from a region of tens of nanometres, limited only by the size of the probe-apex. For graphene, the edges act as a defect itself and alter the electronic behaviour, so when the size of graphene devices inevitably shrinks, the edge properties will dominate. Nanoscale Raman spectroscopy is amongst the handful of techniques that can be used to study devices at this scale. Although many other single-layer 2-D materials have not yet been studied with TERS, reports on measurements using techniques lacking nanoscale resolution reveal that nanoscale Raman and photoluminescence measurements will also enable the investigation of these materials for many potential applications in nanoscale devices.

ACKNOWLEDGEMENTS

AP, SM, NK and DR acknowledge financial support from the Innovation, Research and Development programme of the National Measurement System, UK. NK and DR acknowledge financial support from the EMRP NEW02 project 'Metrology for Raman spectroscopy'. The EMRP is jointly funded by the EMRP participating countries within EURAMET and the European Union. WS acknowledges the financial support from Natural Sciences Foundation of China (Grant No: 61306115 and 61178039), China Postdoctoral Science Foundation (Granted No. 2013M541807) and the International Secondment Scheme from the National Physical Laboratory, UK.

REFERENCES AND NOTES

1. N. Chandrabhas, A.K. Sood, D.V.S. Muthu, C.S. Sundar, A. Bharathi, Y. Hariharan, C.N.R. Rao. Reversible pressure-induced amorphization in solid c-70 - raman and photoluminescence study. *Phys. Rev. Lett.* **1994**, 73, 3411-14.
2. K.S. Subrahmanyam, R. Voggu, A. Govindaraj, C.N.R. Rao. A comparative Raman study of the interaction of electron donor and acceptor molecules with graphene prepared by different methods. *Chem. Phys. Lett.* **2009**, 472, 96-98.
3. R. Gupta, A.K. Sood, R. Mahesh, C.N.R. Rao. Electronic Raman scattering from La_{0.7}Sr_{0.3}MnO₃ exhibiting giant magnetoresistance. *Phys. Rev. B.* **1996**, 54, 14899-902.
4. U. Maitra, K.E. Prasad, U. Ramamurty, C.N.R. Rao. Mechanical properties of nanodiamond-reinforced polymer-matrix composites. *Solid State Commun.* **2009**, 149, 1693-97.
5. K. Biswas, B. Das, C.N.R. Rao. Growth kinetics of ZnO nanorods: Capping-dependent mechanism and other interesting features. *J. Phys. Chem. C* **2008**, 112, 2404-11.
6. E. Betzig, M. Isaacson, A. Lewis. Collection Mode Near-field Scanning Optical Microscopy. *Appl. Phys. Lett.* **1987**, 51, 2088-90.
7. F. Zenhausern, M.P. O'Boyle, H.K. Wickramasinghe. Apertureless Near-field Optical Microscope. *Appl. Phys. Lett.* **1994**, 65, 1623-25.
8. F. Keilmann, B. Knoll. Enhanced Dielectric Contrast in Scattering-type Scanning Near-field Optical Microscopy. *Opt. Comm.* **2000**, 182, 321.
9. J.N. Chen, M. Badioli, P. Alonso-Gonzalez, S. Thongrattanasiri, F. Huth, J. Osmond, M. Spasenovic, A. Centeno *et. al.* Optical nano-imaging of gate-tunable graphene plasmons. *Nature* **2012**, 487, 77-81.
10. R.M. Stockle, Y.D. Suh, V. Deckert, R. Zenobi. Nanoscale chemical analysis by tip-enhanced Raman spectroscopy. *Chem. Phys. Lett.* **2000**, 318, 131-36.
11. N. Hayazawa, Y. Inouye, Z. Sekkat, S. Kawata. Metallized Tip Amplification of Near-field Raman Scattering. *Opt. Commun.* **2000**, 183, 333-36.
12. B. Pettinger, G. Picardi, R. Schuster, G. Ertl. Surface enhanced Raman spectroscopy: Towards single molecular spectroscopy. *Electrochemistry* **2000**, 68, 942-49.
13. M.S. Anderson. Locally enhanced Raman spectroscopy with an atomic force microscope. *Appl. Phys. Lett.* **2000**, 76, 3130-32.
14. B. Hecht, H. Bielefeldt, Y. Inouye, D.W. Pohl, L. Novotny. Facts and Artifacts in Near-field Optical Microscopy. *J. Appl. Phys.* **1997**, 81, 2492-98.
15. D. Roy, J. Wang, M.E. Welland. Nanoscale Imaging of Carbon Nanotubes using Tip Enhanced Raman Spectroscopy in Reflection Mode. *Faraday Discuss.* **2006**, 132, 215-25.
16. K.F. Domke, D. Zhang, B. Pettinger. Toward Raman fingerprints of single dye molecules at atomically smooth Au(111). *J. Am. Chem. Soc.* **2006**, 128, 14721-27.
17. L. Xue, W. Li, G.G. Hoffmann, J.G.P. Goossens, J. Loos, G. de With. High-Resolution Chemical Identification of Polymer Blend Thin Films Using Tip-Enhanced Raman Mapping. *Macromolecules* **2011**, 44, 2852-58.
18. J. Stadler, T. Schmid, R. Zenobi. Nanoscale Chemical Imaging of Single-Layer Graphene. *ACS Nano* **2011**, 5, 8442-48.
19. W. Su, D. Roy. Visualizing Graphene Edges Using Tip-Enhanced Raman Spectroscopy. *J. Vac. Sci. Technol. B* **2013**, 31, 041808.
20. J.C. Meyer, C. Kisielowski, R. Ermi, M.D. Rossell, M.F. Crommie, A. Zettl. Direct Imaging of Lattice Atoms and Topological Defects in Graphene Membranes. *Nano Lett.* **2008**, 8, 3582-86.
21. S.C. O'Hern, M.S.H. Boutilier, J.-C. Idrobo, Y. Song, J. Kong, T. Laoui, M. Atieh, R. Karnik. Selective Ionic Transport through Tunable Subnanometer Pores in Single-Layer Graphene Membranes. *Nano Lett.* **2014**, 14, 1234-41.
22. M.M. Ugeda, I. Brihuega, F. Guinea, J.M. Gómez-Rodríguez. Missing Atom as a Source of Carbon Magnetism. *Phys. Rev. Lett.* **2010**, 104, 096804.
23. A.C. Ferrari. Raman spectroscopy of graphene and graphite: Disorder, electron-phonon coupling, doping and nonadiabatic effects. *Solid State Commun.* **2007**, 143, 47-57.
24. M.M. Lucchese, F. Stavale, E.H. Martins Ferreira, C. Vilani, M.V.O. Moutinho, R.B. Capaz, C.A. Achete, A. Jorio. Quantifying ion-induced defects and Raman relaxation length in graphene. *Carbon* **2010**, 48, 1592-97.
25. L.G. Cancado, A. Jorio, E.H.M. Ferreira, F. Stavale, C.A. Achete, R.B. Capaz, M.V.O. Moutinho, A. Lombardo *et. al.* Quantifying Defects in Graphene via Raman Spectroscopy at Different Excitation Energies. *Nano Lett.* **2011**, 11, 3190-96.
26. F. Banhart, J. Kotakoski, A.V. Krasheninnikov. Structural Defects in Graphene. *ACS Nano* **2011**, 5, 26-41.
27. Q. Yu, L.A. Jauregui, W. Wu, R. Colby, J. Tian, Z. Su, H. Cao, Z. Liu *et. al.* Control and characterization of individual grains and grain boundaries in graphene grown by chemical vapour deposition. *Nat. Mater.* **2011**, 10, 443-49.
28. O.V. Yazyev, S.G. Louie. Topological defects in graphene: Dislocations and grain boundaries. *Phys. Rev. B.* **2010**, 81, 195420.

29. C. Casiraghi, A. Hartschuh, H. Qian, S. Piscanec, C. Georgi, A. Fasoli, K.S. Novoselov, D.M. Basko, A.C. Ferrari. Raman Spectroscopy of Graphene Edges. *Nano Lett.* **2009**, 9, 1433-41.
30. S. Jung, G.M. Rutter, N.N. Klimov, D.B. Newell, I. Calizo, A.R. Hight-Walker, N.B. Zhitenev, J.A. Stroschio. Evolution of microscopic localization in graphene in a magnetic field from scattering resonances to quantum dots. *Nat. Phys.* **2011**, 7, 245-51.
31. F. Müller, H. Sachdev, S. Hüfner, A.J. Pollard, E.W. Perkins, J.C. Russell, P.H. Beton, S. Gsell *et. al.* How Does Graphene Grow? Easy Access to Well-Ordered Graphene Films. *Small* **2009**, 5, 2291-96.
32. M.I. Katsnelson, A.K. Geim. Electron scattering on microscopic corrugations in graphene. *Phil. Trans. Royal Soc. A* **2008**, 366, 195-204.
33. R. Lv, Q. Li, A.R. Botello-Méndez, T. Hayashi, B. Wang, A. Berkdemir, Q. Hao, A.L. Elías *et. al.* Nitrogen-doped graphene: beyond single substitution and enhanced molecular sensing. *Sci. Rep.* **2012**, 2.
34. E. Cruz-Silva, Z.M. Barnett, B.G. Sumpter, V. Meunier. Structural, magnetic, and transport properties of substitutionally doped graphene nanoribbons from first principles. *Phys. Rev. B* **2011**, 83, 155445.
35. S. Niyogi, E. Bekyarova, M.E. Itkis, H. Zhang, K. Shepperd, J. Hicks, M. Sprinkle, C. Berger *et. al.* Spectroscopy of Covalently Functionalized Graphene. *Nano Lett.* **2010**, 10, 4061-66.
36. A. Eckmann, A. Felten, A. Mishchenko, L. Britnell, R. Krupke, K.S. Novoselov, C. Casiraghi. Probing the Nature of Defects in Graphene by Raman Spectroscopy. *Nano Lett.* **2012**, 12, 3925-30.
37. D. Cohen-Tanugi, J.C. Grossman. Water Desalination across Nanoporous Graphene. *Nano Lett.* **2012**, 12, 3602-08.
38. S. Stankovich, D.A. Dikin, G.H.B. Dommett, K.M. Kohlhaas, E.J. Zimney, E.A. Stach, R.D. Piner, S.T. Nguyen, R.S. Ruoff. Graphene-based composite materials. *Nature* **2006**, 442, 282-86.
39. B.J. Schultz, C.J. Patridge, V. Lee, C. Jaye, P.S. Lysaght, C. Smith, J. Barnett, D.A. Fischer *et. al.* Imaging local electronic corrugations and doped regions in graphene. *Nat. Commun.* **2011**, 2, 372.
40. Q.H. Wang, M.C. Hersam. Room-temperature molecular-resolution characterization of self-assembled organic monolayers on epitaxial graphene. *Nat. Chem.* **2009**, 1, 206-11.
41. A.J. Pollard, E.W. Perkins, N.A. Smith, A. Saywell, G. Goretzki, A.G. Phillips, S.P. Argent, H. Sachdev *et. al.* Supramolecular Assemblies Formed on an Epitaxial Graphene Superstructure. *Angew. Chem. Int. Ed.* **2010**, 49, 1794-99.
42. K.S. Kim, Y. Zhao, H. Jang, S.Y. Lee, J.M. Kim, J.-H. Ahn, P. Kim, J.-Y. Choi, B.H. Hong. Large-scale pattern growth of graphene films for stretchable transparent electrodes. *Nature* **2009**, 457, 706-10.
43. A.J. Pollard, R.R. Nair, S.N. Sabki, C.R. Staddon, L.M.A. Perdigo, C.H. Hsu, J.M. Garfitt, S. Gangopadhyay *et. al.* Formation of monolayer graphene by annealing sacrificial nickel thin films. *J. Phys. Chem. C* **2009**, 113, 16565-67.
44. X. Li, W. Cai, J. An, S. Kim, J. Nah, D. Yang, R. Piner, A. Velamakanni *et. al.* Large-Area Synthesis of High-Quality and Uniform Graphene Films on Copper Foils. *Science* **2009**, 342, 1312-14.
45. Y. Shi, C. Hamsen, X. Jia, K.K. Kim, A. Reina, M. Hofmann, A.L. Hsu, K. Zhang *et. al.* Synthesis of Few-Layer Hexagonal Boron Nitride Thin Film by Chemical Vapor Deposition. *Nano Lett.* **2010**, 10, 4134-39.
46. K.H. Lee, H.-J. Shin, J. Lee, I.-y. Lee, G.-H. Kim, J.-Y. Choi, S.-W. Kim. Large-Scale Synthesis of High-Quality Hexagonal Boron Nitride Nanosheets for Large-Area Graphene Electronics. *Nano Lett.* **2012**, 12, 714-18.
47. J.H. Chen, C. Jang, S. Adam, M.S. Fuhrer, E.D. Williams, M. Ishigami. Charged-impurity scattering in graphene. *Nat. Phys.* **2008**, 4, 377-81.
48. A.M. Goossens, V.E. Calado, A. Barreiro, K. Watanabe, T. Taniguchi, L.M.K. Vandersypen. Mechanical cleaning of graphene. *Appl. Phys. Lett.* **2012**, 100, 073110.
49. K.S. Novoselov, D. Jiang, F. Schedin, T.J. Booth, V.V. Khotkevich, S.V. Morozov, A.K. Geim. Two-dimensional atomic crystals. *Proc. Nat. Acad. Sci. USA* **2005**, 102, 10451-53.
50. F. Bonaccorso, A. Lombardo, T. Hasan, Z. Sun, L. Colombo, A.C. Ferrari. Production and processing of graphene and 2d crystals. *Mater. Today* **2012**, 15, 564-89.
51. S.J. Haigh, A. Gholinia, R. Jalil, S. Romani, L. Britnell, D.C. Elias, K.S. Novoselov, L.A. Ponomarenko *et. al.* Cross-sectional imaging of individual layers and buried interfaces of graphene-based heterostructures and superlattices. *Nat. Mater.* **2012**, 11, 764-67.
52. A.K. Geim and I.V. Grigorieva. Van der Waals heterostructures. *Nature* **2013**, 499, 419-425
53. Y.-C. Lin, C.-C. Lu, C.-H. Yeh, C. Jin, K. Suenaga, P.-W. Chiu. Graphene Annealing: How Clean Can It Be? *Nano Lett.* **2011**, 12, 414-19.
54. A. Nourbakhsh, M. Cantoro, A. Klekachev, F. Clemente, B. Sorée, M.H. van der Veen, T. Vosch, A. Stesmans *et. al.* Tuning the Fermi Level of SiO₂-Supported Single-Layer Graphene by Thermal Annealing. *J. Phys. Chem. C* **2010**, 114, 6894-900.
55. C. Blum, L. Opilnik, J.M. Atkin, K. Braun, S.B. Kammer, V. Kravtsov, N. Kumar, S. Lemesko *et. al.* Tip-enhanced Raman spectroscopy - an interlaboratory reproducibility and comparison study. *J. Raman Spectrosc.* **2014**, 45, 22-31.
56. B.S. Yeo, J. Stadler, T. Schmid, R. Zenobi, W.H. Zhang. Tip-enhanced Raman Spectroscopy - Its status, challenges and future directions. *Chem. Phys. Lett.* **2009**, 472, 1-13.
57. X. Wang, D. Zhang, K. Braun, H.J. Egelhaaf, C.J. Brabec, A.J. Meixner. High-Resolution Spectroscopic Mapping of the Chemical Contrast from Nanometer Domains in P3HT:PCBM Organic Blend Films for Solar-Cell Applications. *Adv. Funct. Mater.* **2010**, 20, 492-99.
58. A. Hartschuh, N. Anderson, L. Novotny. Near-field Raman Spectroscopy using Sharp Metal Tip. *J. Microsc.* **2003**, 210, 234-40.
59. R. Bohme, M. Richter, D. Cialla, P. Rosch, V. Deckert, J. Popp. Towards a specific characterisation of components on a cell surface - combined TERS-investigations of lipids and human cells. *J. Raman Spectrosc.* **2009**, 40, 1452-57.
60. R.V. Maximiano, R. Beams, L. Novotny, A. Jorio, L.G. Cancado. Mechanism of near-field Raman enhancement in two-dimensional systems. *Phys. Rev. B* **2012**, 85, 235434.
61. R. Zhang, Y. Zhang, Z.C. Dong, S. Jiang, C. Zhang, L.G. Chen, L. Zhang, Y. Liao *et. al.* Chemical Mapping of a Single Molecule by Plasmon-Enhanced Raman Scattering. *Nature* **2013**, 498, 82-86.
62. W. Zhu, T. Low, V. Perebeinos, A.A. Bol, Y. Zhu, H. Yan, J. Tersoff, P. Avouris. Structure and Electronic Transport in Graphene Wrinkles. *Nano Lett.* **2012**, 12, 3431-36.
63. R. Beams, L.G. Cançado, L. Novotny. Low Temperature Raman Study of the Electron Coherence Length near Graphene Edges. *Nano Lett.* **2011**, 11, 1177-81.
64. B.S. Yeo, T. Schmid, W. Zhang, R. Zenobi. Towards rapid nanoscale chemical analysis using tip-enhanced Raman spectroscopy with Ag-coated dielectric tips. *Anal. Bioanal. Chem.* **2007**, 387, 2655-62.
65. N. Hayazawa, T. Yano, S. Kawata. Highly reproducible tip-enhanced Raman scattering using an oxidized and metallized silicon cantilever tip as a tool for everyone. *J. Raman Spectrosc.* **2012**, 43, 1177-82.
66. R.S. Sundaram, M. Engel, A. Lombardo, R. Krupke, A.C. Ferrari, P. Avouris, M. Steiner. Electroluminescence in Single Layer MoS₂. *Nano Lett.* **2013**, 13, 1416-21.
67. E. Bortchagovsky, T. Schmid, R. Zenobi. Internal standard for tip-enhanced Raman spectroscopy. *Appl. Phys. Lett.* **2013**, 103, 043111.
68. D. Roy, J. Wang, C. Williams. Novel Methodology for Estimating the Enhancement Factor for Tip-Enhanced Raman Spectroscopy. *J. Appl. Phys.* **2009**, 105, 013530.
69. N. Kumar, A. Rae, D. Roy. Accurate measurement of enhancement factor in tip-enhanced Raman spectroscopy through elimination of far-field artefacts. *Appl. Phys. Lett.* **2014**, 104, 123106.
70. K.F. Mak, C. Lee, J. Hone, J. Shan, T.F. Heinz. Atomically Thin MoS₂: A New Direct-Gap Semiconductor. *Phys. Rev. Lett.* **2010**, 105, 136805.
71. A. Splendiani, L. Sun, Y. Zhang, T. Li, J. Kim, C.Y. Chim, G. Galli, F. Wang. Emerging photoluminescence in monolayer MoS₂. *Nano Lett.* **2010**, 10, 1271-5.
72. W. Zhao, R.M. Ribeiro, M. Toh, A. Carvalho, C. Kloc, A.H. Castro Neto, G. Eda. Origin of indirect optical transitions in few-layer MoS₂, WS₂, and WSe₂. *Nano Lett.* **2013**, 13, 5627-34.

73. Z.Y. Zhu, Y.C. Cheng, U. Schwingenschlogl. Giant spin-orbit-induced spin splitting in two-dimensional transition-metal dichalcogenide semiconductors. *Phys. Rev. B* **2011**, *84*, 153402.
74. K.F. Mak, K. He, C. Lee, G.H. Lee, J. Hone, T.F. Heinz, J. Shan. Tightly bound trions in monolayer MoS₂. *Nat. Mater.* **2013**, *12*, 207-11.
75. M. Buscema, G.A. Steele, H.S.J. van der Zant, A. Castellanos-Gomez. The effect of the substrate on the Raman and photoluminescence emission of single layer MoS₂. *Nano Res.* **2014**, *7*, 561-71.
76. D. Sercombe, S. Schwarz, I.I. Tartakovskii, O. Kolosov, O.D. Pozo-Zamudio, F. Liu, B.J. Robinson, E.A. Chekhovich, A.I. Tartakovskii. Optical investigation of the natural electron doping in thin MoS₂ films deposited on dielectric substrates. *Sci. Rep.* **2013**, *3*, 3489.
77. N. Scheuschner, O. Ochedowski, A.-M. Kaulitz, R. Gillen, M. Schleberger, J. Maultzsch. Photoluminescence of freestanding single- and few-layer MoS₂. *Phys. Rev. B* **2014**, *89*, 125406.
78. W. Zhou, X. Zou, S. Najmaei, Z. Liu, Y. Shi, J. Kong, J. Lou, P.M. Ajayan *et al.* Intrinsic Structural Defects in Monolayer Molybdenum Disulfide. *Nano Lett.* **2013**, *13*, 2615-22.
79. A.M. van der Zande, P.Y. Huang, D.A. Chenet, T.C. Berkelbach, Y. You, G.H. Lee, T.F. Heinz, D.R. Reichman *et al.* Grains and grain boundaries in highly crystalline monolayer molybdenum disulfide. *Nat. Mater.* **2013**, *12*, 554-61.
80. H.R. Gutierrez, N. Perea-Lopez, A.L. Elias, A. Berkdemir, B. Wang, R. Lv, F. Lopez-Urias, V.H. Crespi *et al.* Extraordinary room-temperature photoluminescence in triangular WS₂ monolayers. *Nano Lett.* **2013**, *13*, 3447-54.
81. N. Peimyoo, J. Shang, C. Cong, X. Shen, X. Wu, E.K.L. Yeow, T. Yu. Nonblinking, Intense Two-Dimensional Light Emitter: Monolayer WS₂ Triangles. *ACS Nano* **2013**, *7*, 10985-94.
82. H. Nan, Z. Wang, W. Wang, Z. Liang, Y. Lu, Q. Chen, D. He, P.H. Tan *et al.* Strong Photoluminescence Enhancement of MoS₂ through Defect Engineering and Oxygen Bonding. *ACS Nano* **2014**, *8* 5738-45.
83. S. Tongay, J. Suh, C. Ataca, W. Fan, A. Luce, J.S. Kang, J. Liu, C. Ko *et al.* Defects activated photoluminescence in two-dimensional semiconductors: interplay between bound, charged, and free excitons. *Sci. Rep.* **2013**, *3*, 2657.
84. H.-P. Komsa, J. Kotakoski, S. Kurasch, O. Lehtinen, U. Kaiser, A.V. Krasheninnikov. Two-Dimensional Transition Metal Dichalcogenides under Electron Irradiation: Defect Production and Doping. *Phys. Rev. Lett.* **2012**, *109*, 035503.
85. K. He, C. Poole, K.F. Mak, J. Shan. Experimental demonstration of continuous electronic structure tuning via strain in atomically thin MoS₂. *Nano Lett.* **2013**, *13*, 2931-6.
86. B. Hecht, H. Bielefeldt, D.W. Pohl, L. Novotny, H. Heinzelmann. Influence of Detection Conditions on Near-field Optical Imaging. *J. Appl. Phys.* **1998**, *84*, 5873-82.
87. H.J. Conley, B. Wang, J.I. Ziegler, R.F. Haglund, Jr., S.T. Pantelides, K.I. Bolotin. Bandgap Engineering of Strained Monolayer and Bilayer MoS₂. *Nano Lett.* **2013**, *13*, 3626-30.
88. A. Castellanos-Gomez, R. Roldan, E. Cappelluti, M. Buscema, F. Guinea, H.S. van der Zant, G.A. Steele. Local strain engineering in atomically thin MoS₂. *Nano Lett.* **2013**, *13*, 5361-6.
89. Y.Y. Hui, X. Liu, W. Jie, N.Y. Chan, J. Hao, Y.-T. Hsu, L.-J. Li, W. Guo, S.P. Lau. Exceptional Tunability of Band Energy in a Compressively Strained Trilayer MoS₂ Sheet. *ACS Nano* **2013**, *7*, 7126-31.
90. H. Shi, H. Pan, Y.-W. Zhang, B.I. Yakobson. Quasiparticle band structures and optical properties of strained monolayer MoS₂ and WS₂. *Phys. Rev. B* **2013**, *87*, 155304.
91. S. Mouri, Y. Miyauchi, K. Matsuda. Tunable photoluminescence of monolayer MoS₂ via chemical doping. *Nano Lett.* **2013**, *13*, 5944-8.
92. N. Mao, Y. Chen, D. Liu, J. Zhang, L. Xie. Solvatochromic Effect on the Photoluminescence of MoS₂ Monolayers. *Small* **2013**, *9*, 1312-15.
93. Z.-L. Zhang, L. Chen, S.-X. Sheng, M.-T. Sun, H.-R. Zheng, K.-Q. Chen, H.-X. Xu. High-vacuum tip enhanced Raman spectroscopy. *Front. Phys.* **2014**, *9*, 17-24.
94. J.M. Klingsporn, N. Jiang, E.A. Pozzi, M.D. Sonntag, D. Chulhai, T. Seideman, L. Jensen, M.C. Hersam, R.P. Van Duyne. Intramolecular Insight into Adsorbate-Substrate Interactions via Low-Temperature, Ultrahigh-Vacuum Tip-Enhanced Raman Spectroscopy. *J. Am. Chem. Soc.* **2014**, *136*, 3881-87.
95. H. Fu Min, D. Richards. Fluorescence enhancement and energy transfer in apertureless scanning near-field optical microscopy. *J. Opt. A: Pure Appl. Opt.* **2006**, *8*, S234-8.
96. G.M. Lerman, U. Levy. Effect of radial polarization and apodization on spot size under tight focusing conditions. *Opt. Express* **2008**, *16*, 4567-81.
97. N.A. Issa, R. Guckenberger. Fluorescence near metal tips: The roles of energy transfer and surface plasmon polaritons. *Opt. Express* **2007**, *15*, 12131-44.
98. C.A. Barrios, A.V. Malkovskiy, A.M. Kisliuk, A.P. Sokolov, M.D. Foster. Highly Stable, Protected Plasmonic Nanostructures for Tip Enhanced Raman Spectroscopy. *J. Phys. Chem. C* **2009**, *113*, 8158-61.
99. Y.Q. An, J. Rowe, D.B. Dougherty, J.U. Lee, A.C. Diebold. Optical second-harmonic generation induced by electric current in graphene on Si and SiC substrates. *Phys. Rev. B* **2014**, *89*, 115310.
100. N. Kumar, J. Kumar, C. Gerstenkorn, R. Wang, H.-Y. Chiu, A.L. Smirl, H. Zhao. Third harmonic generation in graphene and few-layer graphite films. *Phys. Rev. B* **2013**, *87*, 121406.
101. J.J. Dean, H.M. van Driel. Second harmonic generation from graphene and graphitic films. *Appl. Phys. Lett.* **2009**, *95*, 261910.
102. A.Y. Bykov, P.S. Rusakov, E.D. Obratsova, T.V. Murzina. Probing structural inhomogeneity of graphene layers via nonlinear optical scattering. *Opt. Lett.* **2013**, *38*, 4589-92.
103. X. Yin, Z. Ye, D.A. Chenet, Y. Ye, K. O'Brien, J.C. Hone, X. Zhang. Edge Nonlinear Optics on a MoS₂ Atomic Monolayer. *Science* **2014**, *344*, 488-90.
104. Y. Li, Y. Rao, K.F. Mak, Y. You, S. Wang, C.R. Dean, T.F. Heinz. Probing symmetry properties of few-layer MoS₂ and h-BN by optical second-harmonic generation. *Nano Lett.* **2013**, *13*, 3329-33.
105. K.A. Meyer, K.C. Ng, Z. Gu, Z. Pan, W.B. Whitten, R.W. Shaw. Combined Apertureless Near-Field Optical Second-Harmonic Generation/Atomic Force Microscopy Imaging and Nanoscale Limit of Detection. *Appl. Spectrosc.* **2010**, *64*, 1-7.